第 48 卷第 2 期　　硅　酸　盐　学　报　　Vol. 48，No. 2
2020 年 2 月　　JOURNAL OF THE CHINESE CERAMIC SOCIETY　　February，2020
http://www.gxyb.cbpt.cnki.net　　**DOI**：10.14062/j.issn.0454-5648.20190457

均相溶胶体系合成用于异丙醇脱水的 T 型分子筛膜

刘　义，张慧智，张家友，张　飞，桂　田，胡　娜，陈祥树

(江西师范大学先进材料研究院，分子筛膜材料国家地方联合工程实验室，江西师范大学化学化工学院，南昌 330022)

摘　要：采用均相合成溶胶体系通过两步变温法在廉价莫来石支撑体上制备了厚度为 5 μm 薄且致密的 T 型分子筛膜。考察了均相溶胶体系、合成温度和合成时间对所制备膜的晶体形貌以及渗透汽化的影响。结果表明：最优条件下制备的 T 型分子筛膜在 348 K、水/异丙醇质量比为 10/90 的混合体系中表现的渗透通量和分离因子分别高达 4.3 kg/(m^2·h)和 2 000，且该膜具有良好的重复性和水热稳定性。

关键词：分子筛膜；均相溶胶；两步变温晶化；晶体生长；渗透汽化
中图分类号：TQ028.8　　**文献标志码**：A　　**文章编号**：0454–5648(2020)02–0316–09
网络出版时间：2019–12–13



Preparation of Zeolite T Membranes for Isopropanol Dehydration Using Homogenous Liquid Precursors

LIU Yi, *ZHANG Huizhi*, *ZHANG Jiayou*, *ZHANG Fei*, *GUI Tian*, *HU Na*, *CHEN Xiangshu*
(Institute of Advanced Materials (IAM), State–Province Joint Engineering Laboratory of Zeolite Membrane Materials, College of Chemistry and Chemical Engineering, Jiangxi Normal University, Nanchang 330022, China)

Abstract: Thin and dense zeolite T membranes with a thickness of 5 μm on low-cost mullite tubular supports were synthesized *via* two-stage varying-temperature crystallization (TSVTC) with homogeneous liquid precursors. Effect of precursors on the crystal morphology and pervaporation performance of as-synthesized membranes, and synthesis time/temperature during the two-stage hydrothermal crystallization process was investigated. The results show that zeolite T membranes synthesized under optimized conditions have an enhanced pervaporation performance (*i.e.*, the high flux of 4.3 kg/(m^2·h), and the separation factor of 2 000 in water/isopropanol (10/90, mass ratio) aqueous solution at 348 K). These membranes show a good reproducibility and a long-term hydrothermal stability as well.

Keywords: zeolite membrane; homogeneous liquid precursor; two-stage varying-temperature crystallization; crystal growth; pervaporation

Inorganic zeolite membranes are considered as one of the most promising candidates for organic solvents dehydration by pervaperation (PV) or vapor permeation (VP), which are attributed to their uniform pore structures, selective adsorption and excellent thermal/chemical stability[1–2]. Some studies focused on hydrophilic zeolite membranes for dehydration of organic aqueous mixtures due to the preferential adsorption to water[3–5]. Zeolite NaA membrane has an excellent separation performance in alcohols dehydration, which are industrialized by several commercial companies and academic institutions[6–7]. However, NaA-type zeolite membrane with a maximum aluminum content in the framework (as Si/Al mole ratio=1) shows a poor stability in the dehydration of organic solvents even with traced acid[8].

收稿日期：2019–07–01。　修订日期：2019–08–01。
基金项目：国家国际科技合作专项(2015DFA50190)；国家自然科学基金项目(21868013，21476099 和 21766010)资助项目。
第一作者：刘　义(1994—)，女，硕士研究生。
通信作者：胡　娜(1984—)，女，博士，高级实验师；
陈祥树(1966—)，男，博士，教授。

Received date: 2019–07–01.　**Revised date:** 2019–08–01.
First author: LIU Yi (1994–), female, Master candidate.
E-mail: 274453879@qq.com
Correspondent author: HU Na (1984–), female, Ph.D., Senior Experimentalist; CHEN Xiangshu (1966–), male, Ph.D., Professor.
E-mail: huna@jxnu.edu.cn; cxs66cn@jxnu.edu.cn

Several types of zeolite membranes with a greater framework Si/Al ratio were developed, such as CHA[4,9–10], T[5,11–12], MOR[13–14], and ZSM-5[15], which are suitable alternatives to the dehydration in acidic solutions. Among them, T-type zeolite (OFF−ERI intergrowth) with the effective pore size of 0.36 nm × 0.51 nm and the moderate Si/Al ratio of 3–4 possesses a good hydrophilic property and a superior acid resistance[5,11–12,16–19]. Zeolite T membrane has a high potential for organic solvent dehydration in a moderate acid system (pH value >3)[11,16,18]. Some efforts are taken to the preparation of high-quality zeolite T membranes, *i.e*., seeding operations[17–18], use of macroporous tubes and hollow fibers[11–12,16], and regulation of synthesis systems (OH^- or F^-)[19]. Although the performance of zeolite membrane was considerably improved by the strategies above, it is still a challenge to develop a low-cost and efficient synthesis method of preparing thin and dense zeolite T membrane to meet industrial requirements.

The two-stage varying-temperature crystallization (TSVTC) method is considered as an efficient and economical hydrothermal method, involving the preparation of zeolite powders and membranes such as NaY[20], T[21–22], MFI (ZSM-5)[23–24] and SAPO-34[22]. Compared to the conventional constant temperature crystallization (CCTC) method, the TSVTC method is composed of two hydrothermal crystallization processes conducted at higher and lower temperatures in nucleation and crystallization stages, leading to a shorter crystallization time and a higher membrane intensity[21,23–24]. In a previous work[21], zeolite T membrane prepared by the TSVTC method also exhibited good CO_2 separation properties. Therefore, we would like to extend the TSVTC method to further improve the fluxes of these zeolite T membranes for pervaporation and dehydration of alcohols. This is counterintuitive since one could expect the synthesis time required for well-intergrowth layers to be shorter. It is thus essential to control the synthesis process of sol or gel precursor by the TSVTC method. However, it is rather difficulty to increase the number of nuclei in these precursors. In general, the conventional approach indicates the use of concentrated colloidal solution system under greater supersaturation conditions[25–26]. Some work reported the synthesis of zeolite T membranes at a lower water/silica ratio (*i.e*., less than 25)[5,27–29]. Nevertheless, these precursors obtained through the conventional method ("one-pot" method) could form the heterogeneous gels that are highly viscous and turbid. They pose challenges for homogeneous dispersion, readily impacting the quality of the zeolite layers. The heterogeneous gels are not ideal for the effective synthesis due to their high density gradient.

In this work, we used the hydrolysis of silica source in alkaline hydroxide–water solution prior to the reaction with aluminum sources to provide a homogeneous liquid precursor ("sol"-type) easy to regulate the rates of zeolite nucleation and crystal growth. Thin and dense zeolite T membranes with a thickness of 5 μm on low-cost mullite tubular supports were synthesized *via* two-stage varying-temperature crystallization (TSVTC) with the homogeneous liquid precursors.

1 Experimental

1.1 Materials

Aluminum hydroxide was purchased from Wako Pure Chemical Industries Co., China. Colloidal silica (40%, mass fraction), sodium silicate solution (26.5% SiO_2, 14% Na_2O, respectively), and tetramethylammonium hydroxide solution (25% in water) were purchased from Sigma-Aldrich Co., China. Precipitated silica (VN2) was purchased from Degussa Co., China. Sodium hydroxide (96%) and potassium hydroxide (82%) were purchased from Tianjin Fuchen Chemical Reagent Plant, China. All reagents were invoked as purchased without any further purification. Deionized (DI) water was produced by KM-UPT20UV (Beijing Kingman Technology Co., Ltd., China). Porous mullite tubular support (12 mm in outer diameter, 1.5 mm in thickness, 1.0 μm in average pore size and 10 cm in length) was purchased from Nikkato Co., Japan.

1.2 Zeolite membrane preparation

Seeds preparation and seeding procedure could refer to a previous work[30]. Zeolite T seeds have a column-like shape with 2–4 μm in length[30]. A seed slurry was obtained by mixing 5 g seed powder and 20 g water under ultarsonic pretreatment for 30 min. The outside surface of the supports was rubbed with the seed slurry back and forth for approximately 1 min[10,19,21,30]. The seeded supports were dried at 353 K for 1 h.

Zeolite T membranes were prepared with a homogeneous liquid precursor in varying-temperature crystallization. The precursor was obtained *via* the separate hydrolysis. For the synthesis of zeolite T membrane, precipitated silica as a silica source was dissolved in sodium hydroxide solution, and aluminum hydroxide as an alumina source was simultaneously hydrolyzed in alkaline solution with sodium hydroxide and potassium hydroxide. These two separate solutions were mixed together to form a precursor solution with the molar compositions of SiO_2: $0.015Al_2O_3$:$0.25Na_2O$:$0.08K_2O$:$25H_2O$. In a typical synthesis, 7.0 g sodium hydroxide was dissolved in deionized water under stirring, and then 22.5 g precipitated silica was added into the solution and heated. This leads to a liquid silica designed as solution A. Meanwhile, 0.8 g sodium hydroxide, 0.9 g aluminum hydroxide and 3.9 g potassium hydroxide were dissolved to provide an aluminate solution, which is designed as solution B. Solutions A and B were mixed. Fig. 1(a) shows the schematical of the synthesis procedures. The resultant synthesis solution was aged under stirring at room

temperature for 24 h. The seeded supports were vertically placed in a stainless steel autoclave filled with the synthesis solution above for membrane preparation. The crystallization reaction was initially carried out in an oven preheated to 423 K for a given duration (denoted as "the initial stage"), and then rapidly changed into second stage at 373 K for different durations (denoted as "the final stage"). After the synthesis, the autoclave was cooled down to room temperature and the as-synthesized membranes were washed using DI water for 10–15 min, and soaked into DI water for several times until pH=7.0. The membranes were dried at 353 K for 12 h. Moreover, alternative silica sources such as colloidal silica and sodium silicate were used, and precipitated silica was used as a normal silica source for membrane preparation.

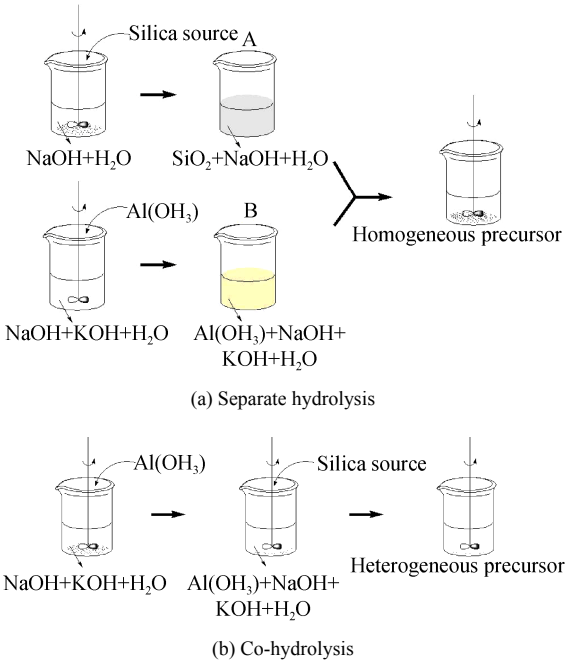


Fig. 1 Procedures for the synthesis precursors derived from different hydrolysis

For comparison purpose, the normal hydrolysis described in a previous work[30] is defined as the co-hydrolysis, which is achieved by adding the silica sources into aluminate solution with some amounts of H_2O, NaOH and KOH (see Fig.1 (b)) under other fixed conditions. All the precursors derived from different silica sources were coded as Sample #*n* (*n* denotes the run number).

1.3 Characterization and PV test

The crystalline phases of the membranous crystals were characterized by a model Ultima IV X-ray diffractor with a Cu-K_α radiation source (Rigaku Co. Ltd., Japan). The XRD patterns were recorded at a scanning rate of 4(°)/min in the 2θ range of 5°–45°, and the relative crystallinity was calculated by the percentage of the sum of the corresponding XRD peaks intensities of the desired sample at 2θ 7.7°, 13.3° and 20.3° to those of the standard sample under the optimal conditions. The morphologies of zeolite layers were determined by a model SU8020 scanning electron microscope (Hitachi Co., Japan). The particle size in the aged precursors was determined by a model Nano-ZS dynamic light scattering particle sizer (Malvern Co. Ltd., UK). The FT-IR spectra were measured in the wavenumber range of 650–4 000 cm^{-1} in a model Nicolet 6700 FT-IR spectroscope (Thermo Co., USA).

The pervaporation (PV) performance of zeolite membranes was evaluated with water/isopropanol (IPA) mixtures using a PV experimental apparatus[10,30]. The effective area of the membrane was 28 cm^2 and the permeation side was kept in vacuum at 100 Pa. The PV separation performance of zeolite membrane was evaluated *via* the permeation total flux (J_t, kg/(m^2·h)) and the separation factor (α). The permeation flux is defined as $J_t=m_t/(At)$, where m_t (kg) is the total mass of the permeation collected by a liquid-nitrogen trap, A (m^2) is the effective membrane area, and t (h) is the test time, respectively. The separation factor is defined as $\alpha=(Y_A/Y_B)/(X_A/X_B)$, where X_A, X_B, Y_A and Y_B are the mass fractions of components A (H_2O) and B (IPA) in the feed and permeate, respectively. X_A, X_B, Y_A and Y_B were analyzed by a model GC-2014C gas chromatograph instrument (Shimadzu Co. Ltd., Japan) equipped with 3 m column packed with Polarpack Q poly (ethyleneglycol)-1000.

2 Results and discussion

2.1 Precursors

Table 1 shows the pervaporation performance of zeolite membranes (M1–M6) prepared from different synthesis precursors. The membrane (M1) prepared *via* the separate hydrolysis of precipitated silica as a silica source exhibits a high permeation flux of (4.3±0.03) kg/(m^2·h) and a good separation factor of 2 000±220, which is better than that *via* the co-hydrolysis (M4). The membranes (M2–M3, M5–M6) prepared using colloidal silica and sodium silicate *via* the hydrolysis above show a poor separation factor.

Figure 2 shows the XRD patterns of zeolite membranes (M1–M6) obtained by different hydrolysis of alternative silica sources such as precipitate silica, colloidal silica and sodium silicate. The XRD peaks of six membranes are composed of the characteristic peaks of reported T-type framework and mullite support[17,27,30], indicating that these membranes all are a pure T-type phase. These results indicate that the precursors derived from various silica sources under different hydrolysis can affect the quality of zeolite layers rather than the crystalline phase of the membranous crystals.

To verify the distinctiveness of hydrolysis, we selected precipitated silica, and evaluated potential differences of the homogeneous precursors. Figure 3 shows the results of the DLS performed on representative

samples (#1 and #4) derived from the separate hydrolysis and co-hydrolysis of precipitated silica, respectively. For the separate hydrolysis (Sample #1), the light diffusing object of fresh sol is 60 nm that is too small to be identified, indicating the nanoparticles are formed. The DLS value increases slowly as the aging time increases from 0 h to 12 h, proving that aging under stirring leads to the aggregation of primary particles in solution. However, the particle size centered at approximately 120 nm appears for 12 h aging, and subsequently remains constant when the time extends to 24 h. From the corresponding IR analysis results (see Fig. 4 (a)), the siloxane (Si–O–Si) stretch region at 1 105 cm^{-1} and 796 cm^{-1} and Si–OH stretching vibration band at 970 cm^{-1} of precipitated silica[31] immediately transform into a distinct peak at 1 020 cm^{-1} assigned to the siloxane (Si–O–Si) due to the increase of Si–O–Na, when a silicate liquid is obtained from the hydrolysis of precipitated silica in NaOH aqueous solution (solution A in Fig. 1 (a). This typical peak at 1 020 cm^{-1} does not change much until the sol is well aged. Thus, the pH value and the ionic conductivity of this precursor do not change with the increase of aging time (see Fig. 5). The similar phenomenon was also reported[31]. Those results indicate that Sample #1 consists mainly of ionic oligomeric silicate and aluminosilicate species, and most aggregates of these primary particles are formed within the first aging for 12 h, then the more aggregates were already nucleated when the size of growing particles reaches a plateau beyond 12 h.

Table 1　Pervaporation performance of zeolite T membranes prepared from alternative silica sources toward water/isopropanol (10/90) aqueous solution at 348 K

Membrane Co.	Precursor	Silica source	Hydrolysis pretreatment	Precursor before aging	Pervaporation performance	
					J_t/(kg·m^{-2}·h^{-1})	$\alpha_{H_2O/IPA}$
M1	Sample#1	Precipitated silica	Separate hydrolysis	Clear	4.3±0.03	2000±220
M2	Sample#2	Sodium silicate	Separate hydrolysis	Clear	High	1
M3	Sample#3	Colloidal silica	Separate hydrolysis	Clear	3.6±0.03	230±35
M4	Sample#4	Precipitated silica	Co-hydrolysis	Milk-like	3.0±0.04	250±40
M5	Sample#5	Sodium silicate	Co-hydrolysis	Milk-like	High	1
M6	Sample#6	Colloidal silica	Co-hydrolysis	Milk-like	2.9±0.10	300±50

Note: Membrane sol composition: $1SiO_2$:$0.015Al_2O_3$:$0.25Na_2O$:$0.08K_2O$:$25H_2O$; Synthesis conditions: the initial stage at 423 K for 2 h, the final stage at 373 K for 10 h. J_t is permeation flux α is separation factor.

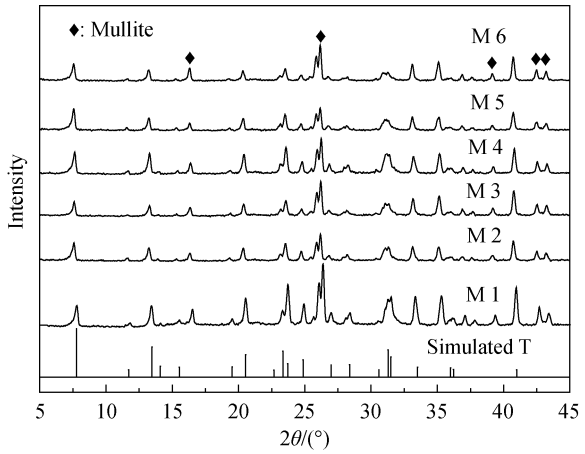


Fig. 2　XRD patterns of zeolite membranes M1−M6 prepared from different precursors

However, for the co-hydrolysis (Sample #4), the DLS value reduces linearly as the aging time increases from 0 h to 12 h, then kept a constant value until the sol is aged for 24 h. It is indicated that precipitated silica is dissolved as the aging time increases, the depletion of hydroxide ions reduces the solution pH value and the ionic conductivity[32], which is also consistent with the aging time changes in pH value and ionic conductivity of Sample #4 in Table 1 (see Fig. 5). The IR analysis results (see Fig. 4 (b)) show the distinct differences. A small peak at 970 cm^{-1} localized Si–OH stretching mode appears only while other bands of precipitate silica disappear in the fresh gel of Sample #4. When the aging time prolongs to 6 h, this peak at 970 cm^{-1} shifts gradually toward 1 020 cm^{-1}, promoting the polymerization equilibrium of silicate species from Si–OH bond to siloxane (Si–O–Si(Al)). Afterwards, the peak at 1 020 cm^{-1} does not change.

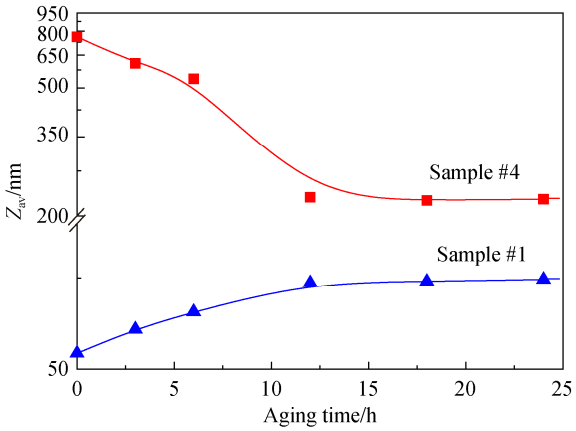
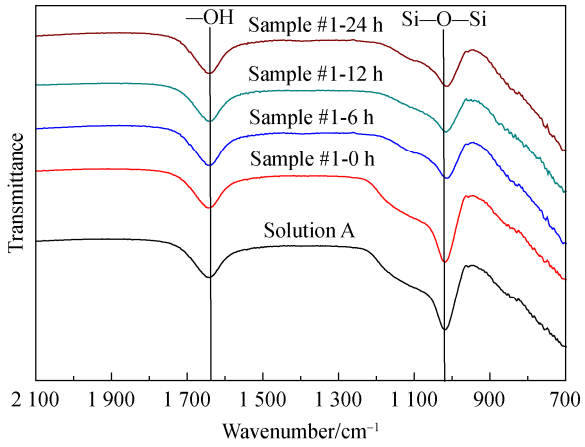
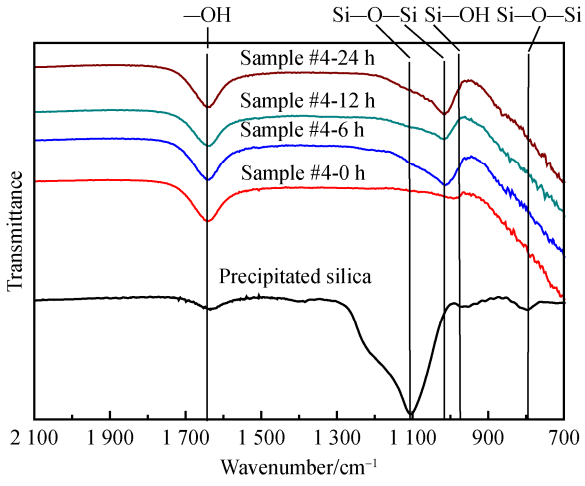


Fig. 3　Results of DLS measurement on synthesis precursors after aging at room temperature for different time



(a) Sample #1 in Table 1



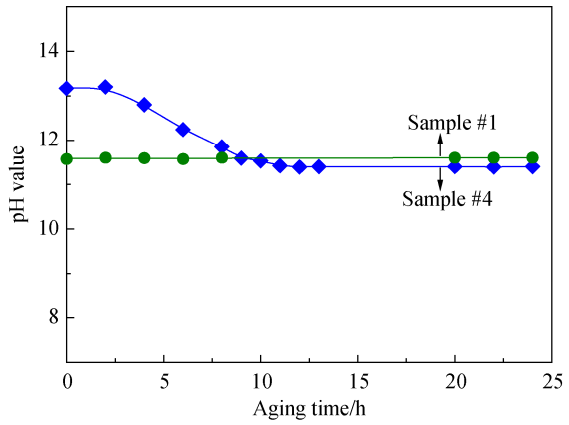
(b) Sample #4 in Table 1

Fig. 4 FT-IR spectra of different synthesis precursors after aging for different time

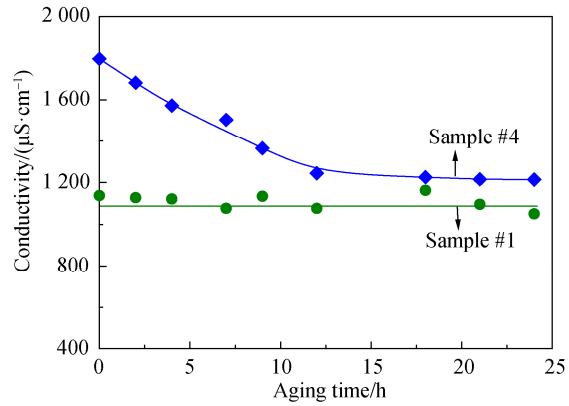
Therefore, the evolution between different hydrolysis of precipitate silica reflects a disparity, which is obtained *via* the aggregation in the early stage of aging process of the former precursor (Sample #1), compared to the dissolution from the latter precursor (Sample #4). Meanwhile, the final particle size of Sample #4 is almost 2 times greater than that of Sample #1. It is assumed that all silica could be converted to precursor after aging, and the number density of nucleation centers in Sample #4 would be 6.1 times smaller than that in Sample #1. Therefore, the aggregation of homogeneous liquid derived from the separate hydrolysis of precipitate silica in NaOH–H_2O solution favors increasing the number of nucleation centers, and thus improving the quality of zeolite layers, which coincides with the results of their pervaporation performances in Table 1.

2.2 Crystallization process in the homogeneous liquid precursors

Table 2 shows the synthesis conditions for membrane preparation by the CCTC and TSVTC method with the standard precursor sol (Sample #1). Figure 6 shows the crystallization processes of T-type zeolite membrane prepared by the CCTC at higher (M7–M11 in Table 2) and lower synthesis temperatures (M12–M16 in Table 2), respectively. The membrane with a high crystalline density (M9) can be obtained from hydrothermal synthesis at 423 K for 6 h, while the membrane (M14) needs 24 h at a lower temperature of 373 K. The nucleation rate at a higher temperature is much faster than that at a lower temperature, indicating that the higher synthesis temperature gives the more effective nuclei in zeolite crystallization. However, a higher synthesis temperature may result in the formation of larger crystals, which is easily to form larger intercrystalline defects. Massive boundary defects among larger crystals appear on the surface of the membranes prepared for 4 h and even for 8 h (M8 and M10 in Table 2, as shown in Figs. 7 (a) and 7 (b), resulting in a poor separation factor for water/isopropanol. Moreover, the separation performance of the membrane prepared at 373 K improves when the synthesis time increases from 24 h to 36 h (M14–M16 in Table 2), which can be attributed to the improvement of membrane intergrowth (see Figs. 7 (c) and 7 (d)). This phenomenon is also consistent with the results in the crystallization of other crystals[20,25,33].



(a) pH value



(b) Ionic conductivity

Fig. 5 pH value and ionic conductivity of synthesis precursor obtained from Samples #1 and #4 (Table 1) after aging for a given time

Table 2　Synthesis conditions and pervaporation performances of as-synthesized membranes toward water/isopropanol (10/90) aqueous solution at 348 K

Membrane	Synthesis conditions[a]	Pervaporation Performance	
		J_{total}/(kg·m^{-2}·h^{-1})	$\alpha_{H2O/IPA}$
M1	423 K for 2 h and 373 K for 10 h	4.3	2 000
M7	423 K for 2 h	High	1
M8	423 K for 4 h	3.9	800
M9	423 K for 6 h	3.6	520
M10	423 K for 8 h	3.2	450
M11	423 K for 12 h	2.9	600
M12	373 K for 8 h	3.4	200
M13	373 K for 20 h	3.3	500
M14	373 K for 24 h	3.7	650
M15	373 K for 32 h	3.9	1 000
M16	373 K for 36 h	3.3	950
M17	423 K for 4 h and 373 K for8 h	4.6	200
M18	423 K for 2 h and 373 K for 8 h	3.7	850
M19	423 K for 2 h and 373 K for 12 h	3.4	140

Note: [a]: Sample #1: $1SiO_2$:$0.015Al_2O_3$:$0.25Na_2O$:$0.08K_2O$:$25H_2O$.

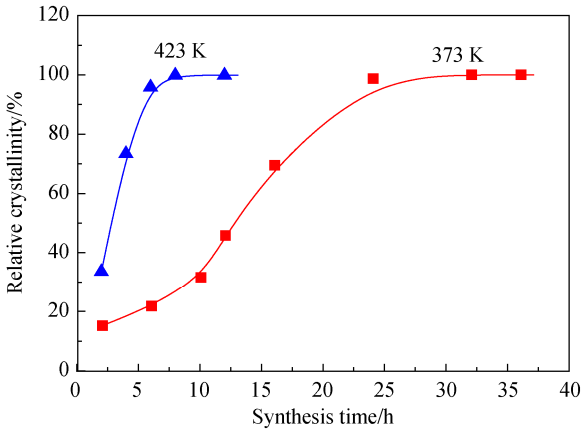
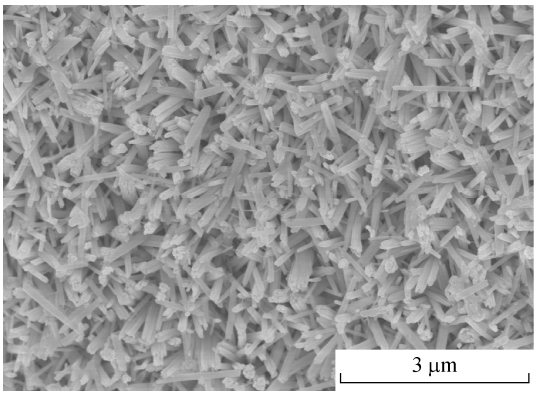
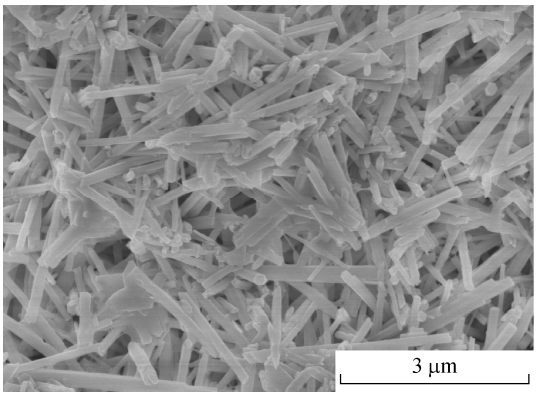


Fig. 6　Crystallization curves of zeolite membranes by the CCTC method

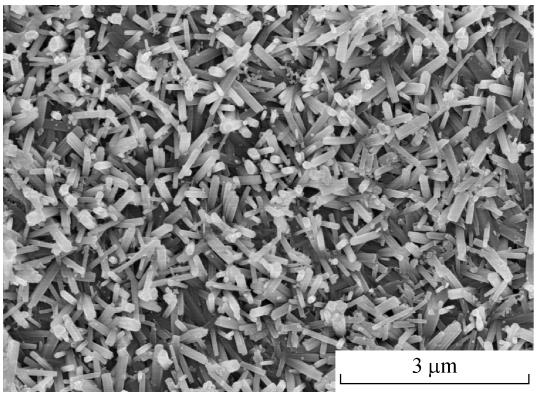
To reduce the crystallization time and obtain highly-quality zeolite T membranes, the two stage varying-temperature crystallization (TSVTC) method was used in membrane preparation. In the TSVTC process, the initial stage at a higher temperature (423 K) was carried out to accelerate the nucleation, and the final stage at a lower temperature (373 K) was carried out to control the crystal size at a low crystallization rate[20–21,25]. Figure 8 shows the SEM images of zeolite T membranes prepared by the TSVTC method for different synthesis time. Some rod-like crystals are loosely packed on the support surface after the hydrothermal synthesis at 423 K only for 2 h, whereas massive voids exist between crystals at this stage (see Fig. 8 (a)). The crystallization process continues to the final stage, which the membrane



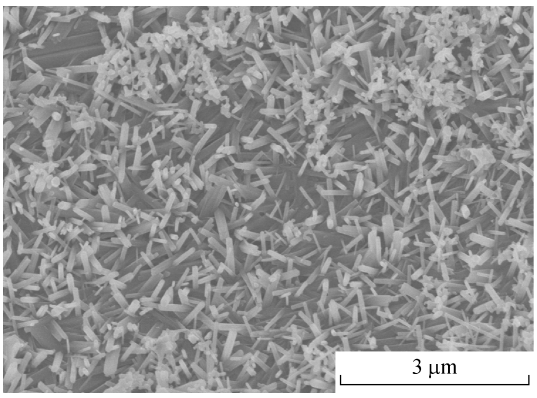
(a) Surface of M8 in Table 2



(b) Surface of M10 in Table 2

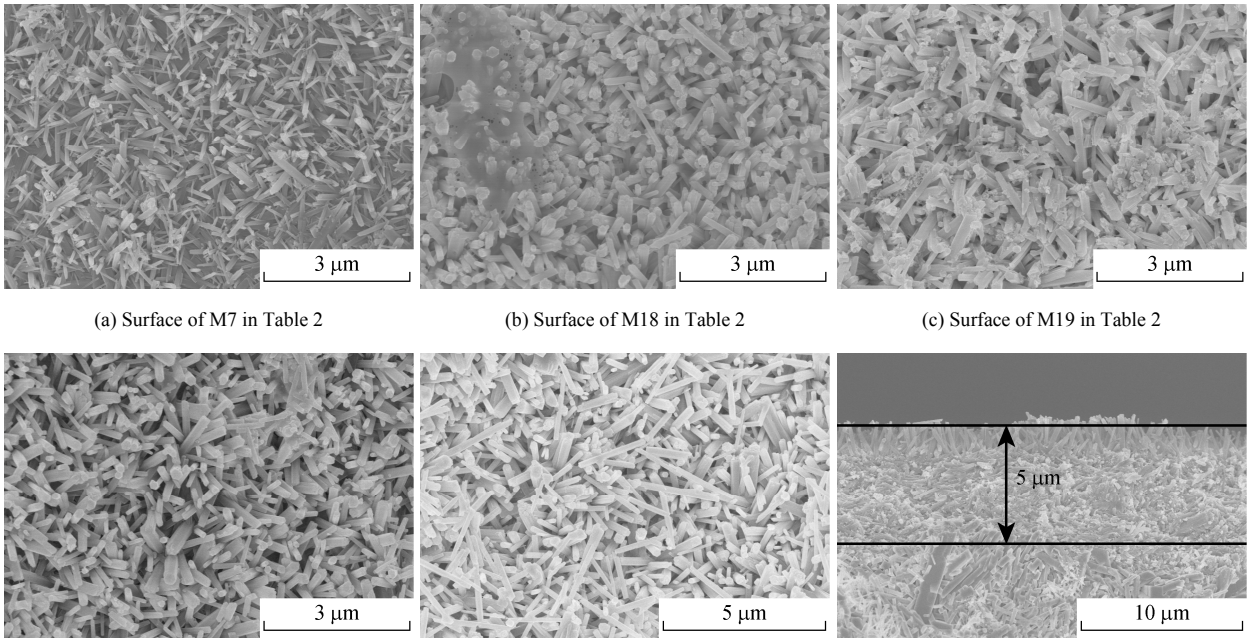


(c) Surface of M14 in Table 2



(d) Surface of M16 in Table 2

Fig. 7　Surface SEM images of zeolite membranes synthesized by CCTC method for different synthesis time



(a) Surface of M7 in Table 2 (b) Surface of M18 in Table 2 (c) Surface of M19 in Table 2

(d) Surface of M17 in Table 2 (e) Surface of M1 in Table 1 (f) Cross section of M1 in Table 1

Fig. 8 SEM images of zeolite membranes synthesized by TSVTC method for different synthesis time

is kept at 373 K for 8 h (M18). Most of zeolite crystals are perpendicularly grown onto the surface of support, followed by the formation of their gaps (see Fig. 8 (b)). The density of crystals increases and they become crowded when the synthesis time increases to 10 h at the final stage (M1) (see Fig. 8 (e)). The membrane thickness is 5 μm, as shown in Fig. 8f. At the synthesis time of 12 h (M19), zeolite T crystals grow wider due to their overgrowth and consequently developed column-like and randomly oriented crystals with some defects at their perimeters (see Fig. 8 (c)), resulting in the decrease of separation factor. The nuclei thus grow into larger crystals when nucleated at 423 K for 2 h and upon crystallization at 373 K for 10 h. Membrane M17 (the initial stage at 423 K for 4 h, the final stage at 373 K for 8 h) has a decreased separation factor, indicating the formation of boundary defects among the crystals due to the overgrowth, as shown in Fig. 8 (d). Zeolite T membrane (M1) prepared at optimized synthesis temperature and time (*i.e.*, the initial stage at 423 K for 2 h, the final stage at 373 K for 10 h) has a high flux of 4.3 kg/(m^2·h) and a high separation factor of 2000 toward a 90% (mass fraction) isopropanol aqueous solution at 348 K.

2.3 Membrane synthesis reproducibility and long-term test stability

Figure 9 shows ten membranes prepared with the homogeneous liquid by the TSVTC method under optimized synthesis conditions. The PV performance of these membranes has the similar values, *i.e.*, the average flux is (4.1±0.11) kg/(m^2·h) and the separation factor is 2 100±320, respectively. The standard deviation values of their fluxes and separation factors are relatively low (*i.e.*, 2.68% and 15.24%), indicating that membrane preparation with the homogeneous liquid by the TSVTC method has a reasonable reproducibility.

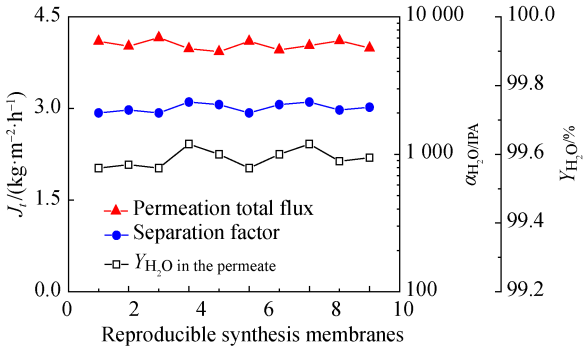


Fig. 9 PV performances of zeolite T membranes prepared under optimized synthesis condition toward 90% isopropanol solution at 348 K

Figure 10 shows the time-course variations in the permeation total flux and separation factor of zeolite T membrane under optimized synthesis conditions for a 70% isopropanol aqueous solution at 348 K. The PV operations were continuously carried out during 7-d test to investigate the hydrothermal stability. The fluxes and separation factors of T-type zeolite membrane do not obviously changed, as shown in Fig.10. The membrane has a stable flux of approximately 6.9 kg/(m^2·h) and a separation factor of 850 (water content in permeate side of 99.72%). The similar result was also obatined in a previous study[10,30]. These results indicate that this membrane could have a good hydrothermal stability for the dehydration of water-rich solution in a lab-scale long-term test.

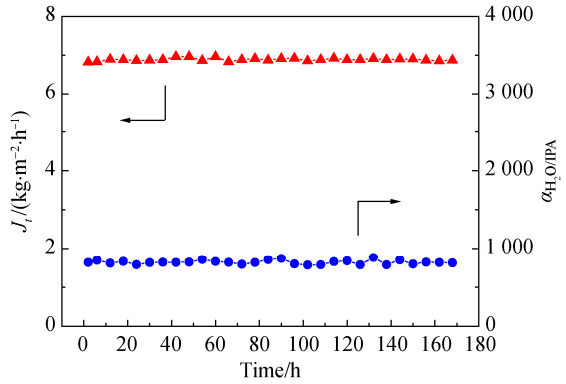


Fig. 10　Time-course of the permeation total flux and separation factor of zeolite T membrane toward 70% isopropanol aqueous solution at 348 K

2.4　Comparison to the literatures

Table 3 shows the separation results of typical fluoride-free zeolite T membranes for a 90% isopropanol solution at 348 K. All the zeolite T membranes have a water/isopropanol separation factor of greater than 2000 (water content in permeate side is higher than 99.55%) in the standard test system. Wang *et al*[12] reported that zeolite T membranes using α-Al_2O_3 hollow fibers supports have a flux of 14.3 kg/(m^2·h). The usage of this support is favorable for a high flux due to its thinner wall and higher porosity although the synthesis time is 24 h. Note that the high-performance T-type zeolite membrane through epitaxial growth using the same hollow fibers supports in a reported literature[11] could be attributed to the same membrane thickness (3–4 μm) as that of the seed layer, while the flux of their macroporous alumina supported membrane prepared under the same synthesis conditions was only 5.9 kg/(m^2·h). A previous work reported that zeolite T membranes on the low-cost mullite supports using micro-sized seeds by the CCTC method[30]. The membrane had a high flux of 2.5 kg/(m^2·h). In this work, we introduced a novel and inexpensive route for the synthesis of T-type zeolite membranes with the homogeneous liquid precursor by the TSVTC method. The current membrane (M1) has an improved flux of 4.3 kg/(m^2·h) and a considerable separation factor, which is 70% greater than the previous membranes[30], and it consumes only one third of the former synthesis time (35 h). Compared to other reported zeolite T membranes using the same mullite support in the literatures[18,27,30], the flux of the membranes is much higher, and the synthesis time is shorter, which are available to industrial implementation of membrane separation due to the reduced cost and reasonable reproducibility.

Table 3　Comparison of pervaporation performances of zeolite T membranes toward water/isopropanol (10/90) aqueous solution at 348 K

Support		Synthesis conditions			Pervaporation performance		Ref.
Type	Pore size/μm	Silica source	Temperature/K	Time/h	J_t/(kg·m^{-2}·h^{-1})	$\alpha_{H_2O/IPA}$	
Al_2O_3	3–4	Colloidal silica	423	4	5.9	>10000	[11]
α–Al_2O_3 hollow fibers	0.3	Fumed silicate	373	24	14.3	>10000	[12]
α–Al_2O_3	2–3	Colloidal silica	373	30	2.5	10000	[17]
Mullite[a]	0.6	Colloidal silica	378	35	1.2	2040	[18]
Mullite	1.3	Precipitated silica	373	30	2.2	8900	[27]
α–Al_2O_3[b]	2–3	Colloidal silica	428	6	1.4	2318	[28]
Mullite	1.0	Colloidal silica	423	35	2.5	13000	[30]
Mullite	1.0	Precipitated silica[c]	423+373	2+10	4.3	2000	This work

Note: [a]: Pervaporation test was measured at 348 K toward water/ethanol with mass ratio as 10/90 mixtures; [b]: Pervaporation test was measured at 343 K toward water/isopropanol with mass ratio as 10/90 mixtures; [c]: The separate hydrolysis of silica source and alumina source.

3　Conclusions

An improved strategy was proposed based on the homogeneous precursors from separate hydrolysis for a two-stage varying-temperature synthesis of high-quality zeolite T membranes. The results indicated that the duration of as-synthesized membrane was shorten by 65% and the flux of this membrane was increased by 70% in comparison to those of previous fluoride-free membrane at a constant temperature, which were attributed to the improvement of their nucleation and crystallization with the homogeneous precursor and the thinner membrane obtained from two-stage hydrothermal crystallization process. Ten membranes obtained under the optimized synthesis conditions exhibited an average flux of 4.3 kg/(m^2·h) and a separation factor of 2 000 (water content in permeate side was higher than 99.55%) toward 90% isopropanol aqueous solution at 348 K, respectively. The reasonable reproducibility and long-term hydrothermal stabilities were given for the synthesized membranes. This strategy could provide an effective method for wide industrial implementation of membrane separation.

References:

[1] VANHOOF V, VAN DE ABEELE L, BUEKENHOUDT A, et al. Economic comparison between azeptropic distillation and different hybrid systems combining distillation with pervaporation for the dehydration of isopropanol[J]. Sep Purif Technol, 2004, 37: 33–49.

[2] LIN Y S. Microporous and dense inorganic membranes: current status and prospective[J]. Sep Purif Technol, 2001, 25: 39–55.

[3] CHAPMAN P D, OLIVEIRA T, LIVINGSTON A G, et al. Membranes for the dehydration of solvents by pervaporation[J]. J Membr Sci, 2008, 318: 5–37.

[4] HASEGAWA Y, ABE C, NISHIOKA N, et al. Influence of synthesis gel composition on morphology, composition, and dehydration performance of CHA-type zeolite membranes[J]. J Membr Sci, 2010, 363: 256–264.

[5] CUI Y, KITA H, OKAMOTO K I. Zeolite T membrane: preparation, characterization, pervaporation of water/organic liquid mixtures and acid stability[J]. J Membr Sci, 2004, 236: 17–27.

[6] MORIGAMI Y, KONDO M, ABE J, et al. The first large-scale pervaporation plant using tubular-type module with zeolite NaA membrane[J]. Sep Purif Technol, 2001, 25: 251–260.

[7] WANG J C, YE P, GAO X C, et al. Modeling investigation of geometric size effect on pervaporation dehydration through scaled-up hollow fiber NaA zeolite membranes[J]. Chin J Chem Eng, 2018, 26: 1477–1484.

[8] SCHERZER J. The preparation and characterization of aluminum deficient zeolites[J]. Catal Mater, 1984, 248: 157–200.

[9] JIANG J, WANG X R, PENG L, et al. Batch-scale preparation of hollow fiber supported CHA zeolite membranes and module for solvents dehydration[J]. Micropor Mesopor Mater, 2017, 250: 18–26.

[10] HU N, LI Y Q, ZHONG S L, et al. Fluoride-mediated synthesis of high-flux chabazite membranes for pervaporation of ethanol using reusable macroporous stainless steel tubes[J]. J Membr Sci, 2016, 510: 91–100.

[11] LUO Y W, LV Y J, KUMAR P, et al. Epitaxial growth: rapid synthesis of highly permeable and selective zeolite-T membranes[J]. J Mater Chem A, 2017, 5: 17828–17832.

[12] WANG R, MA N K, YAN Y S, et al. Ultrasonic-assisted fabrication of high flux T-type zeolite membranes on alumina hollow fibers[J]. J Membr Sci, 2018, 548: 676–684.

[13] LI Y Q, ZHU M H, HU N, et al. Scale-up of high performance mordenite membranes for dehydration of water-acetic acid mixtures[J]. J Membr Sci, 2018, 564: 174–183.

[14] ZHANF Y Q, NAKASAKA Y, TAGO T, et al. Preparation and optimization of mordenite nanocrystal-layered membrane for dehydration by pervaporation[J]. Micropor Mesopor Mater, 2015, 207: 39–45.

[15] FU D L, SCHMIDT J E, PLETCHER P, et al. Uniformly oriented zeolite ZSM-5 membranes with tunable wettability on a porous ceramic[J]. Angew Chem Int Ed, 2018, 57: 12458–12462.

[16] JI M M, GAO X C, WANG X R, et al. An ensemble synthesis strategy for fabrication of hollow fiber T-type zeolite membrane modules[J]. J Membr Sci, 2018, 563: 460–469.

[17] CHEN X X, WANG J Q, YIN D H, et al. High performance zeolite T membrane for dehydration of organics by a new varying temperature hot-dip coating method[J]. AIChE J, 2013, 59: 936–947.

[18] WANG X R, YANG Z Z, YU C L, et al. Preparation of T-type zeolite membranes using a dip-coating seeding suspension containing colloidal SiO_2[J]. Micropor Mesopor Mater, 2014, 197: 17–25.

[19] ZHANG F, ZHENG Y H, HU L L, et al. Preparation of high-flux zeolite T membranes using reusable macroporous stainless steel supports in fluoride media[J]. J Membr Sci, 2014, 456: 107–116.

[20] WANG Z Z, KUMAKIRI I, TANAKA K, et al. NaY zeolite membranes with high performance prepared by a variable-temperature synthesis[J]. Micropor Mesopor Mater, 2013, 182: 250–258.

[21] ZHANG X L, QIU L F, DING M Z, et al. Preparation of zeolite T membranes by a two-step temperature process for CO_2 separation[J]. Ind Eng Chem Res, 2013, 52: 16364−16374.

[22] YIN X Y, CHU N B, LU X W, et al. Cost-effective two-stage varying-temperature rapid crystallization of zeolite T and SAPO-34[J]. J Cryst Growth, 2016, 441: 1–11.

[23] LI Y S, ZHANG X F, WANG J Q, et al. Preparation for ZSM-5 membranes by a two-stage varying-temperature synthesis[J]. Sep Purif Technol, 2001, 25: 459–466.

[24] KONG C L, LU J M, YANG J H, et al. Preparation of silicalite-1 membranes on stainless steel supports by a two-stage varying-temperature in situ synthesis[J]. J Membr Sci, 2006, 285: 258–264.

[25] NAKRANI D, BELANI M, BAJAJ H C, et al. Concentrated colloidal solution system for preparation of uniform Zeolite-Y nanocrystals and their gas adsorption properties[J]. Micropor Mesopor Mater, 2017, 241: 274–284.

[26] OLEKSIAK M D, SOLTIS J A, CONATO M T, et al. Nucleation of FAU and LTA zeolites from heterogeneous aluminosilicate precursors[J]. Chem Mater, 2016, 28: 4906–4916.

[27] CUI Y, KITA H, OKAMOTO K I. Preparation and gas separation performance of zeolite T membrane[J]. J Mater Chem, 2004, 14: 924–932.

[28] ZHANG Q P, ZHOU Z H, WU H D, et al. Optimization of preparing zeolite T membranes from clear Solutions[J]. J Chin Ceram Soc, 2017, 45: 968–975.

[29] ZHOU H, LI Y S, ZHU G Q, et al. Microwave-assisted hydrothermal synthesis of a&b-oriented zeolite T membranes and their pervaporation properties[J]. Sep Purif Technol, 2009, 65: 164–172.

[30] ZHOU R F, HU L L, ZHANG Y J, et al. Synthesis of oriented zeolite T membranes from clear solutions and their pervaporation properties[J]. Micropor Mesopor Mater, 2013, 174: 81–89.

[31] HSU C Y, CHIANG A S T, SELVIN R, et al. Rapid synthesis of MFI zeolite nanocrystals[J]. J Phys Chem B, 2005, 109: 18804–18814.

[32] LI R, LINARES N, SUTJIANTO J G, CHAWLA A, et al. Ultrasmall zeolite L crystals prepared from highly-interdispersed alkali-silicate precursors[J]. Angew Chem Int Ed, 2018, 57: 11283–11288.

[33] KIM S D, NOH S H, PARK J W, et al. Organic-free synthesis of ZSM-5 with narrow crystal size distribution using two-step temperature process[J]. Micropor Mesopor Mater, 2006, 92: 181–188.